Global-mean precipitation and black carbon in AR4 simulations

A. G. Pendergrass and D. L. Hartmann[1]

D. L. Hartmann, Department of Atmospheric Sciences, University of Washington, Box 351640, Seattle, WA 98195, USA. (dhartm@washington.edu)

A. G. Pendergrass, Department of Atmospheric Sciences, University of Washington, Box 351640, Seattle, WA 98195, USA. (angie@atmos.washington.edu)

[1]Department of Atmospheric Sciences,

University of Washington, Seattle,

Washington, USA.

How much and why precipitation changes as the climate warms is uncertain, even for the global mean. In the 21st Century of the IPCC AR4 A1b forcing scenario, global-mean precipitation increase per degree warming varies among models by over a factor of three. Clear-sky atmospheric shortwave absorption change explains over half of the intermodel spread ($r^2 = 0.61$) in precipitation increase. Removing the part of clear-sky atmospheric shortwave absorption change due to water vapor increase reveals that shortwave absorption forcing decreases in NCAR CCSM 3.0 but increases in GFDL CM 2.1, which we attribute to differences in black carbon forcing reported by these modeling groups. The range of applied forcing causes a range in atmospheric shortwave absorption increase, which leads to spread in precipitation increase. In contrast, in the CO_2-doubling forcing scenario, clear-sky atmospheric shortwave absorption explains an insignificant amount of spread ($r^2 = 0.04$).

1. Introduction

How and why does global-mean precipitation change with global warming? The hydrologic cycle transfers heat from the surface to the atmosphere: evaporation cools the surface and precipitation warms the atmosphere through the release of latent heat. The atmosphere cools primarily by radiatively. The rate of precipitation change in the global mean thus depends on the energy budgets of the surface and atmosphere. When greenhouse gas (GHG) concentrations increase in isolation, the surface warms, and evaporation and precipitation generally increase. The increase in the availability of energy for evaporation at the surface and the ability of the atmosphere to radiate away heat limit the amount of precipitation increase [*Allen and Ingram*, 2002]. *Held and Soden* [2006] showed that in the the Intergovernmental Panel on Climate Change (IPCC) Fourth Assessment Report [AR4**,** *Solomon et al.*, 2007] Special Report on Emission Scenarios [SRES, *Nakićenović and Swart*, 2000] A1b forcing experiment, global-mean precipitation increases by 1-3% per degree of global-mean surface temperature increase. This inter-model spread in precipitation response corresponds to 1.6 W m^{-2} K^{-1}. What causes this large range in precipitation response?

Reflecting aerosols in the atmosphere decrease the amount of shortwave (SW) radiation reaching the surface, which both cools the surface and decreases the amount of energy available for evaporation. The effects of absorbing aerosols vary with their height, but they decrease precipitation in most cases [*Ming et al.*, 2010]; their effect on surface temperature is smaller than the effect of reflecting aerosols or GHGs [*Shiogama et al.*, 2010a]. The

additional SW absorption adds heat directly to the atmosphere, which causes a decrease in the latent heating that would otherwise occur.

How precipitation varies across AR4 forcing scenarios was the focus of two recent studies. *Shiogama et al.* [2010b] found that changes in global-mean precipitation depend on the emissions scenario, with black carbon showing a significant effect, but their surface energy budget perspective precluded an explanation. *Frieler et al.* [2011] determined that precipitation changes across AR4 scenarios and models can be skillfully predicted from longwave (LW) and SW absorption and global-mean surface temperature change.

Increased black carbon forcing results in decreased global-mean precipitation in most but not all modeling studies. Black carbon also affects surface temperature, but this effect is small. *Shiogama et al.* [2010a] compared integrations of the Model for Interdisciplinary Research on Climate (MIROC) separately forced with GHGs, black carbon, and sulfate aerosols, and found that black carbon forcing decreases precipitation. *Roberts and Jones* [2004] used the Hadley Center climate model (HadSM4) with online chemistry to find a very slight increase in global-mean precipitation at equilibrium with black carbon forcing, which is inconsistent with other studies. *Andrews et al.* [2010] updated *Roberts and Jones* [2004] using a newer version of the Hadley Center model (HadGEM1) and found that black carbon forcing decreases precipitation.

Here we explore how black carbon forcing influences the intermodel spread in global-mean precipitation change in IPCC AR4. We focus on two models and the A1b forcing scenario in order to explore in depth one reason why global-mean precipitation varies among models.

2. Data

For this study, we use data from the World Climate Research Programme's (WCRP's) Coupled Model Intercomparison Project phase 3 (CMIP3) multi-model dataset [*Meehl et al.*, 2007a]. Variables include surface air temperature (T), precipitation (P), total-sky and clear-sky LW and SW upwelling and downwelling radiation at the surface and upwelling radiation at the top-of-atmosphere (TOA) for models where these fields are available. Clear-sky downwelling LW radiation at the surface is not available for National Center for Atmospheric Research Community Climate System Model 3.0 (CCSM3). Only the first ensemble member for each model is shown. In models with multiple ensemble members, the additional members have similar changes in precipitation and temperature to the first. For each variable and each model, the area-weighted global means are taken and the differences between twenty-year means of the monthly data from the beginning (2011-2030) and end (2080-2099) of the 21st-Century are computed (indicated by Δ). Atmospheric SW absorption is calculated by adding surface upwelling and TOA downwelling and subtracting surface downwelling and TOA upwelling; LW cooling is the same calculation with all signs reversed. Atmospheric SW absorption and LW cooling are normalized by the difference in global-mean surface temperature (ΔT). L is the latent heat of vaporization of water, which we multiply by ΔP for comparison with energetic changes. $L\Delta P/\Delta T$ computed in this way is the hydrologic sensitivity. Table 1 lists the models in descending order of $L\Delta P/\Delta T$, which varies from 2.1 to 0.57 W m^{-2} K^{-1} (a factor of 3.7).

3. Changes in global-mean precipitation and components of the atmospheric energy budget

Figure 1 shows $L\Delta P/\Delta T$ plotted against changes in clear-sky atmospheric SW absorption, clear-sky atmospheric LW cooling, and changes in LW and SW cloud radiative forcing (the difference between the total- and clear-sky radiative fields). If GHG forcing and water vapor feedback cause changes in precipitation, then precipitation change should correlate well with the changes in atmospheric LW cooling. While clear-sky atmospheric LW cooling change does explain most of the increase in $L\Delta P$ when it is not normalized by ΔT ($r = 0.73$, $r^2 = 0.53$, not shown), it correlates poorly with $L\Delta P/\Delta T$ (Figure 1c). This is because water vapor concentration depends strongly on temperature and largely determines clear-sky atmospheric LW cooling; normalizing by ΔT removes this dependence. Often, we think that intermodel spread in AR4 simulations is dominated by clouds; however, Figure 1b and d show no significant relationship between $L\Delta P/\Delta T$ and changes in SW or LW cloud radiative forcing. On the other hand, $L\Delta P/\Delta T$ correlates well with changes in clear-sky atmospheric SW absorption, explaining over half of the intermodel spread ($r = -0.78$, $r^2 = 0.61$).

4. Patterns of change in clear-sky atmospheric SW absorption

Water vapor and absorbing aerosols are the main SW absorbers in the troposphere expected to change in the next century, aside from clouds. To explore how clear-sky atmospheric SW absorption changes in the 21st Century, we focus on two of the AR4 models: the model with the greatest precipitation increase and smallest increase in clear-sky atmospheric SW absorption, CCSM3, and the model with the smallest precipitation

increase and largest increase in clear-sky atmospheric SW absorption, Geophysical Fluid Dynamics Laboratory Coupled Model 2.1 (CM2.1).

Figure 2 shows A1b scenario 21st-Century change in clear-sky atmospheric SW absorption for CCSM3 and CM2.1. In CCSM3 SW absorption decreases, except in limited regions over the Tropics, while in CM2.1 it increases almost everywhere. Using feedback kernels for atmospheric column radiation from *Previdi* [2010], we remove the increase in absorption due to water vapor concentration increase. *Previdi* [2010] showed this calculation for four models from AR4 A1b, including CM2.0 and CM2.1, but not for CCSM3. The residual change in clear-sky SW absorption (total minus increased water vapor absorption) strongly resembles the spatial pattern of anthropogenic absorbing aerosol emissions. Tropospheric ozone changes have not been accounted for in this analysis, but these effects are likely to be small because fractional changes of tropospheric ozone in the 21st Century are small [*Wigley et al.*, 2002]. The sign of the residual change is negative in CCSM3 and positive in CM2.1.

5. The timeseries of black carbon forcing

The treatment of aerosols in IPCC AR4 model runs was documented in Table 10.1 of *Meehl et al.* [2007b]. While the SRES scenarios specified GHG and sulfate aerosol emissions, they did not specify the black carbon forcing. Modeling groups took different approaches to incorporating black carbon forcing in the 21st Century. Most models did not include it at all; the ones that did are bold in Table 1. CCSM3 scaled the present geographical concentrations of black carbon by projections of global mean sulfate (SO_x) aerosol burden, reported in *Meehl et al.* [2006]. In contrast, an atmospheric chemistry model was

used in CM2.0 and CM2.1 (CM2) to interactively calculate concentrations of black carbon [*Horowitz et al.*, 2003]. Concentrations of black carbon closely follow emissions because black carbon is short-lived in the atmosphere [*Horowitz*, 2006]. The present-day spatial pattern of black carbon emissions scaled by the timeseries of global-mean carbon monoxide (CO) burden drove the chemistry model in CM2 according to *Levy et al.* [2008]. We obtain the SO_x and CO timeseries from 2000 to 2100 from the A1 scenario of the Asian Pacific Integrated Model (AIM) scenario from SRES [http:www.grida.no/climate/ipcc/emission, accessed 8/31/2011, *Nakićenović and Swart*, 2000]; the bottom left panel of Figure 3 shows them converted to black carbon timeseries following *Meehl et al.* [2006] for CCSM3 and *Levy et al.* [2008] for CM2. In CCSM3, black carbon increased until 2020 and then declined for the remainder of the century, ending lower than the 2000 values. In CM2, the emissions increased slowly but steadily throughout the century, nearly doubling from 2000 to 2100. The top left panel of Fig. 3 shows the timeseries of the clear-sky SW absorption with the contribution from water vapor removed. For CM2, the steady increase in absorption with time corresponds to what is expected if the black carbon emission timeseries is comparable to its forcing timeseries. For CCSM3, the residual SW absorption increases until around 2030 as expected, but it does not decrease substantially below the 2000 values, as would be expected from the black carbon forcing timeseries.

SW absorption and precipitation should respond to time-dependent aerosol changes; we test whether they do by comparing timeseries of black carbon forcing, clear-sky atmospheric SW absorption, and precipitation for CM2 and CCSM3 (Figure 3). The timeseries are smoothed once with a 1-2-1 weighted average filter [*Gonzalez and Woods*, 2002]

for display purposes. In CM2.0 and CM2.1, precipitation increased slowly and steadily throughout the century, at a rate of 0.15 W m^{-2} dec^{-1}. In CCSM3, it increased slowly at first, though not as slowly as in CM2 (0.2 W m^{-2} dec^{-1} from 2000-2020), rapidly around mid-century (0.6 W m^{-2} dec^{-1} from 2030-2070), and slowly again at the end of the century (0.05 W m^{-2} dec^{-1} from 2080-2100). The overall increase was large (3.5 W m^{-2}). For the atmosphere to maintain energy balance, an increase in SW absorption must be compensated by an increase in LW cooling or a decrease in sensible or latent heating. The precipitation responses in CCSM3 and CM2 are consistent with this expectation. A large increase in precipitation ($L\Delta P$=3.5 W m^{-2}) accompanied the decrease in SW absorption (-1.0 W m^2) by aerosols in CCSM3 (though net increase in SW absorption occurred due to increased water vapor), while only modest increases in precipitation (1 W m^{-2}) accompanied the increase in SW absorption by aerosols in CM2 (1.7 W m^{-2}). Observational estimates of black carbon forcing on atmospheric absorption are much larger than the global-mean of the residuals shown here. *Ramanathan and Carmichael* [2008] estimate the present-day black carbon forcing of atmospheric absorption to be 2.6 W m^{-2}, and *Chung et al.* [2005] estimate that it is 3.0 W m^{-2}; however, these estimates are highly uncertain.

The other models shown in Figure 1 and Table 1 that incorporated black carbon changes in AR4 simulations are MIROC medres, MIROC hires, and HadGEM3. They fall just in the bottom half of simulations in terms of $L\Delta P/\Delta T$, and they all contain indirect effects of aerosols. Indirect effects are expected to mitigate the direct effects on precipitation by increasing reflection of SW to space via cloud brightening and by decreasing the precipi-

tation efficiency of clouds [*Chuang et al.*, 2002]. Both of these indirect effects are a result of the decreased size of cloud droplets that occurs when the number of cloud condensation nuclei increases [see review by *Lohmann and Feichter*, 2005]. However, the indirect effect of black carbon is not expected to be large. The semi-direct effect, which is the decrease in cloud cover due to aerosol heating [*Ackerman et al.*, 2000], is included in all simulations but does not affect the clear-sky radiation.

6. Contrast with CO_2-doubling scenario

If differences in absorbing aerosol forcing cause the intermodel spread in $L\Delta P/\Delta T$, scenarios without changes in absorbing aerosols should have less spread in clear-sky atmospheric SW absorption and $L\Delta P/\Delta T$. For the carbon dioxide (CO_2)-doubling scenario, precipitation, surface air temperature, and clear-sky SW upwelling and downwelling radiation at the surface and upwelling at the TOA are obtained from the WCRP CMIP3 database for the same models as above for the "1pctto2x" scenario, except for the Canadian Center for Climate Modeling and Analysis GCM (CCCMA CGCM3.1 T63), which has insufficient data for this scenario. The 1pctto2x scenario is also a transient simulation coupled to a full ocean, so it is the most appropriate scenario to compare to A1b. Differences are taken between decadal averages of years 60-69 and 1-10. Other calculations are the same as for the A1b scenario.

Figure 4 shows $L\Delta P/\Delta T$ plotted against clear-sky atmospheric SW absorption per degree change in global-mean surface temperature for CO_2-doubling scenario. There is almost no relationship between clear-sky atmospheric SW absorption change and $L\Delta P/\Delta T$, in stark contrast to the A1b scenario (Figure 1a). This lack of relationship is consistent

with the absorbing aerosol forcing in A1b driving the intermodel spread in precipitation. The range of $L\Delta P/\Delta T$ in the CO_2-doubling scenario is 0.8 W $m^{-2}K^{-1}$, while for A1b the range was 1.5 W $m^{-2}K^{-1}$. The smaller but still substantial range of $L\Delta P/\Delta T$ in the CO_2-doubling scenario indicates that variability in precipitation stems from sources other than absorbing aerosol forcing. This is consistent with clear-sky shortwave atmospheric absorption explaining half of the variance in $L\Delta P/\Delta T$ ($r^2 = 0.61$).

7. Conclusions

The IPCC AR4 dataset, and in particular the A1b scenario, have been widely used to study how and why precipitation could change this century. In this study, we compare global-mean precipitation change and atmospheric radiation budget components, and we find that clear-sky shortwave absorption is highly correlated with precipitation change. We examine the spatial pattern of clear-sky SW absorption change in NCAR CCSM 3.0 and GFDL CM 2.1, and we find that it resembles the spatial pattern of anthropogenic aerosol emissions, but increases in GFDL CM2.1 and decreases in NCAR CCSM 3.0. We compare timeseries of black carbon forcing from those models with clear-sky atmospheric SW absorption, absorption with the increase due to water vapor increase removed, and precipitation, and find that the timeseries of precipitation change for CCSM3 and CM2 are consistent with the idea that clear-sky shortwave absorption drives precipitation changes, as would be expected from simple radiative-convective equilibrium. Finally, we compare global-mean precipitation and clear-sky atmospheric SW absorption from the CO_2-doubling scenario, and find that in this scenario precipitation change does not correlate with clear-sky shortwave absorption. This indicates that black carbon forc-

ing differences explain a substantial portion, but not all, of the intermodel spread in global-mean precipitation in the A1b scenario of AR4. Details of the forcings in AR4, in particular the black carbon forcing, were left unspecified in the emissions scenarios, and forcing data was not available in a coordinated way, which is why this source of spread has gone unappreciated for some time.

Black carbon is short lived, so it is plausible that it could continue to increase throughout the century, or alternatively it could decrease. It is useful to explore a wide range of possibilities including both increases and decreases in black carbon to capture a range of potential future trajectories. Studies making use of A1b projections should take into account the effects that black carbon forcing has on precipitation, including in this dataset. In the future, model intercomparison studies that might be used to investigate precipitation changes should document and report black carbon forcing.

Acknowledgments. This work was funded by grant NSF AGS - 0960497. We acknowledge the modeling groups, the WCRP's Working Group on Coupled Modeling (WGCM) for their roles in making available the WCRP CMIP3 multi-model dataset. Support of this dataset is provided by the Office of Science, U.S. Department of Energy. Michael Previdi kindly provided his feedback kernel data. Dargan Frierson provided helpful suggestions that improved the work. Three anonymous reviewers provided feedback that improved the manuscript.

References

Ackerman, A. S., O. B. Toon, D. E. Stevens, A. J. Heymsfield, V. Ramanathan, and E. J. Welton (2000), Reduction of tropical cloudiness by soot, *Science*, *288*, 1042–1047, doi:10.1126/science.288.5468.1042.

Allen, M. R., and W. J. Ingram (2002), Constraints on future changes in climate and the hydrologic cycle, *Nature*, *419*(6903), 224–232, doi:10.1038/Nature01092.

Andrews, T., P. M. Forster, O. Boucher, N. Bellouin, and A. Jones (2010), Precipitation, radiative forcing and global temperature change, *Geophys. Res. Lett.*, *37*, 5 pp., doi: 201010.1029/2010GL043991.

Chuang, C., J. Penner, J. Prospero, K. Grant, G. Rau, and K. Kawamoto (2002), Cloud susceptibility and the first aerosol indirect forcing: Sensitivity to black carbon and aerosol concentrations, *J. Geophys. Res.*, *107*(D21), 45–64.

Chung, C. E., V. Ramanathan, D. Kim, and I. A. Podgorny (2005), Global anthropogenic aerosol direct forcing derived from satellite and ground-based observations, *J. Geophys. Res.*, *110*, D24207, doi:10.1029/2005JD006356.

Frieler, K., M. Meinshausen, T. Schneider von Deimling, T. Andrews, and P. Forster (2011), Changes in global-mean precipitation in response to warming, greenhouse gas forcing and black carbon, *Geophysical Research Letters*, *38*, 5 pp., doi: 201110.1029/2010GL045953.

Held, I., and B. Soden (2006), Robust responses of the hydrological cycle to global warming, *J. Climate*, *19*(21), 5686–5699.

Horowitz, L. W. (2006), Past, present, and future concentrations of tropospheric ozone and aerosols: Methodology, ozone evaluation, and sensitivity to aerosol wet removal, *J. Geophys. Res.*, *111*(D22), D22211.

Horowitz, L. W., et al. (2003), A global simulation of tropospheric ozone and related tracers: Description and evaluation of MOZART, version 2, *J. Geophys. Res.*, *108*(D24), 4784, doi:10.1029/2002JD002853.

Gonzalez, R. C., and R. E. Woods (2002), *Digital image processing*, 2nd ed., 793 pp, Prentice Hall, Upper Saddle River, NJ.

Levy, I. I. H., M. D. Schwarzkopf, L. Horowitz, V. Ramaswamy, and K. L. Findell (2008), Strong sensitivity of late 21st century climate to projected changes in short-lived air pollutants, *J. Geophys. Res.*, *113*(D6), D06102, doi:10.1029/2007JD009176.

Lohmann, U., and J. Feichter (2005), Global indirect aerosol effects: a review, *Atmos. Chem. Phys*, *5*, 715–737.

Meehl, G. A., et al. (2006), Climate change projections for the twenty-first century and climate change commitment in the CCSM3, *J. Climate*, *19*, 2597–2616.

Meehl, G. A., C. Covey, K. E. Taylor, T. Delworth, R. J. Stouffer, M. Latif, B. Mcavaney, and J. F. Mitchell (2007a), The WCRP CMIP3 multimodel dataset: A new era in climate change research, *Bull. Amer. Meteorol. Soc.*, *88*(9), 1383–1394.

Meehl, G.A., et al. (2007b), Global climate projections, in *Climate Change 2007: The Physical Science Basis. Contribution Of Working Group I To The Fourth Assessment Report Of The Intergovernmental Panel On Climate Change*, edited by S. Solomon et al., Cambridge Univ. Press, Cambridge, U. K. and New York, NY, USA.

Ming, Y., V. Ramaswamy, and G. Persad (2010), Two opposing effects of absorbing aerosols on global-mean precipitation, *Geophys. Res. Lett.*, *37*(13), doi: 10.1029/2010GL042895.

Nakićenović, N., et al. (Eds.) (2000), *Special Report On Emissions Scenarios. A Special Report Of Working Group III Of The Intergovernmental Panel On Climate Change.*, 599 pp., Cambridge Univ. Press, Cambridge, U. K. And New York, NY, USA.

Previdi, M. (2010), Radiative feedbacks on global precipitation, *Environ. Res. Lett.*, *5*, 025,211.

Ramanathan, V., and G. Carmichael (2008), Global and regional climate changes due to black carbon, *Nature Geosci*, *1*(4), 221–227, doi:10.1038/Ngeo156.

Roberts, D. L., and A. Jones (2004), Climate sensitivity to black carbon aerosol from fossil fuel combustion, *J. Geophys. Res.*, *109*(D16), D16,202.

Shiogama, H., S. Emori, K. Takahashi, T. Nagashima, T. Ogura, T. Nozawa, T. Takemura (2010a), Emission scenario dependency of precipitation on global warming in the MIROC3.2 model, *J. Climate*, *23*, 2404-2417.

Shiogama, H., et al. (2010b), Emission scenario dependencies in climate change assessments of the hydrological cycle, *Clim. Change*, *99*(1), 321–329, doi:10.1007/S10584-009-9765-1.

Solomon, S., et al. (Eds.) (2007), *Climate Change 2007: The Physical Science Basis. Contribution Of Working Group I To The Fourth Assessment Report Of The Intergovernmental Panel On Climate Change*, Cambridge Univ. Press, Cambridge, U. K. and New York, NY, USA.

Wigley, T. M. L., S. J. Smith, and M. J. Prather (2002), Radiative forcing due to reactive gas emissions. *J. Climate*, *15*(18), 2690-2696.

Table 1. Models ranked by $L\Delta P/\Delta T$ in the 21st Century of IPCC AR4 A1b scenario, and their changes in global-mean precipitation and total-sky SW absorption. Boldfaced models include black carbon forcing [Table 10.1, *Solomon et al.*, 2007].

HS rank	Model name	$L\Delta P/\Delta T$ (W m^{-2} K^{-1})	$L\Delta P$ (W m^{-2})	ΔSW (W m^{-2})
1	**NCAR CCSM3.0**	2.1	3.5	0.094
2	MRI CGCM2.3.2A	1.8	3.2	0.47
3	IPSL CM4	1.8	4	2.5
4	MPI ECHAM5	1.8	4.7	2.7
5	CCCMA CGCM3.1	1.6	2.6	1.9
6	CCCMA CGCM3.1 T63	1.6	3.3	2.1
7	CNRM CM3	1.6	3.1	2.1
8	INMCM3.0	1.4	2.2	0.88
9	**MIROC3.2 HiRes**	1.4	4.3	3.8
10	**MIROC3.2 MedRes**	1.4	3.3	3.2
11	**UKMO HadGEM1**	1.1	2.6	4
12	MIUB ECHO G	0.98	2.1	3
13	UKMO HadCM3	0.88	1.9	2.6
14	**GFDL CM2.0**	0.73	1.5	3.7
15	**GFDL CM2.1**	0.57	1	3.4

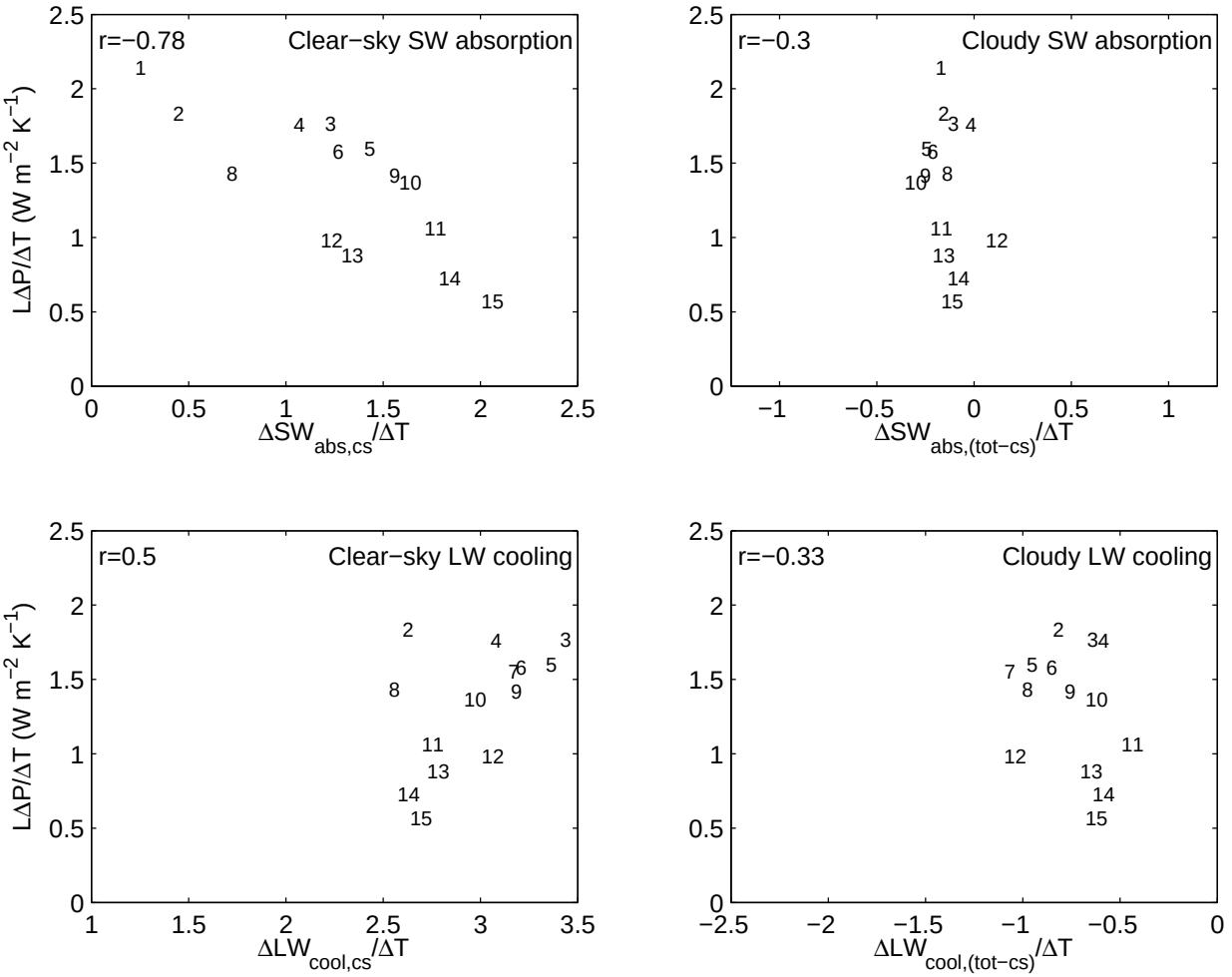

Figure 1. IPCC AR4 A1b forcing scenario 21st-Century changes in global-mean precipitation, clear-sky atmospheric SW absorption and LW cooling and SW and LW cloud radiative forcing per degree global-mean surface temperature change. See Table 1 for model key. LW cooling data is not available for Model 1.

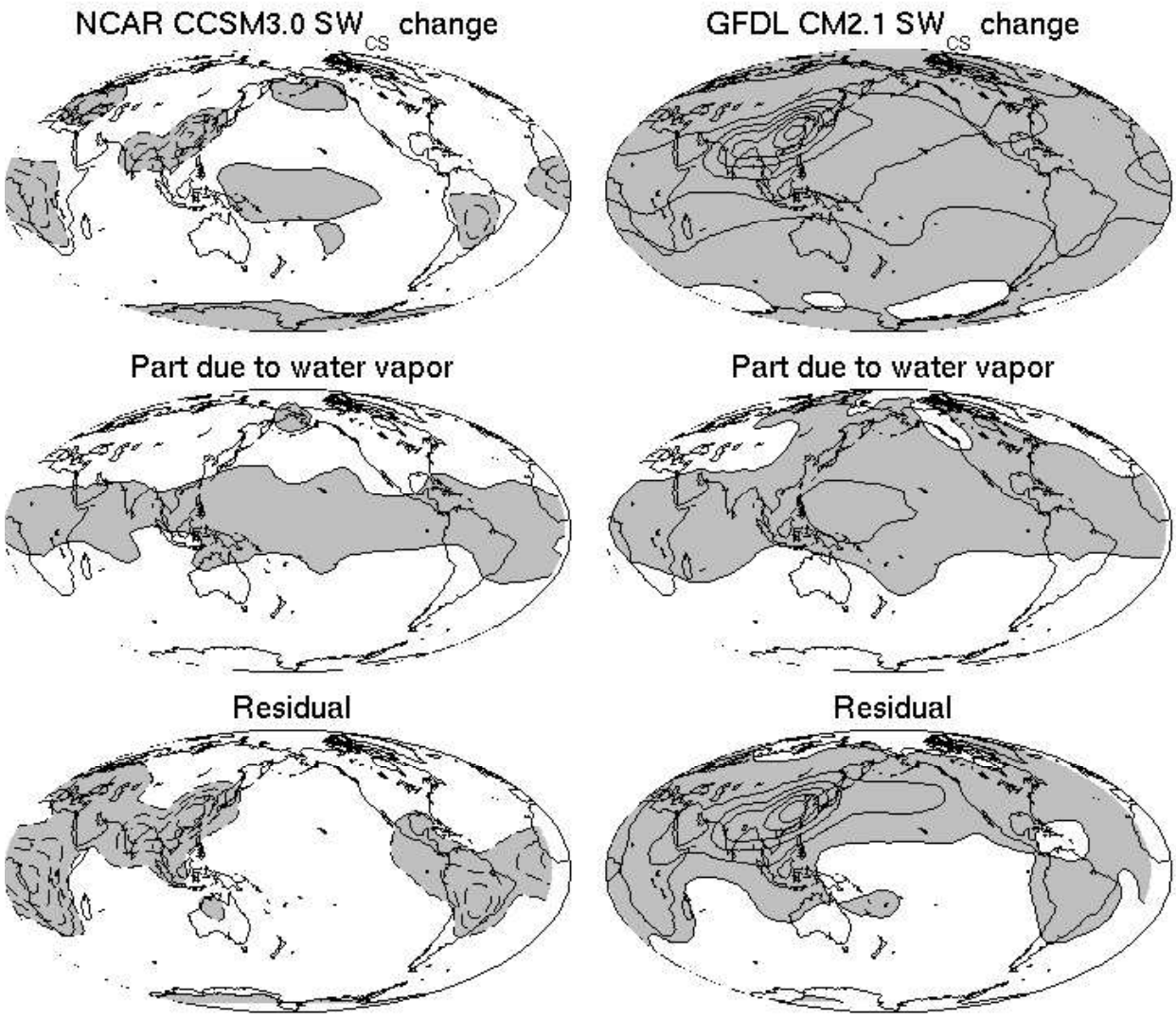

Figure 2. Change in clear-sky atmospheric SW absorption in A1b scenario for the 21st century of (left) NCAR CCSM 3 and (right) GFDL CM 2.1. (Top) Clear-sky atmospheric SW absorption change. (Middle) Part of clear-sky atmospheric SW absorption change due to water vapor increase, calculated with radiative kernels from *Previdi* [2010]. (Bottom) Residual change in clear-sky atmospheric SW absorption. Solid contours are positive changes and dashed contours are negative changes; contour interval is 1.5 W m^{-2}; and shaded areas are at least 1.5 W m^{-2} different from zero. Global mean of bottom left panel is -1.0 W m^{-2} and bottom right is 1.7 W m^{-2}.

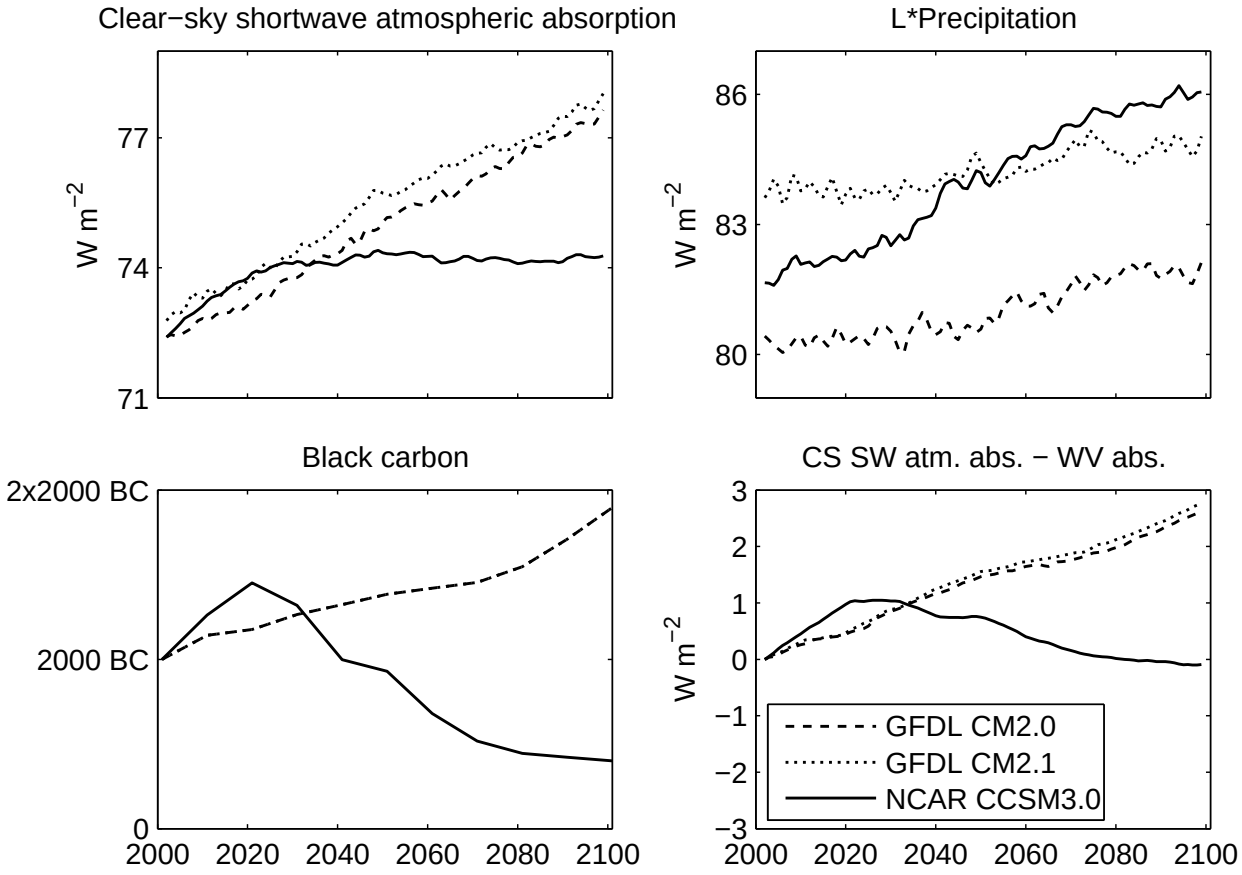

Figure 3. Clear-sky SW absorption, clear-sky SW absorption with water vapor contribution removed, precipitation, and black carbon forcing for GFDL CM 2.0, 2.1, and NCAR CCSM 3.0, smoothed once using a 1-2-1 filter [*Gonzalez and Woods*, 2002]. Black carbon forcing is the timeseries of global mean A1b CO (GFDL CM2.0 and CM2.1 black carbon emissions) and SO_x (NCAR CCSM 3.0 black carbon concentrations).

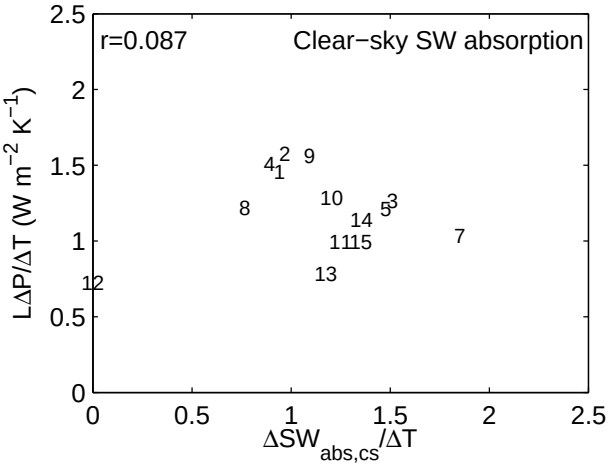

Figure 4. Changes in global-mean precipitation and clear-sky atmospheric SW absorption per degree global-mean surface temperature change for CO_2-doubling experiments. See Table 1 for model key. Changes are calculated between years (60-70) and (0-10). Compare to the top-left panel of Fig. 1.